Spatial–Temporal Distribution of Whisker-Evoked Activity in Rat Somatosensory Cortex and the Coding of Stimulus Location

Rasmus S. Petersen[1] **and Mathew E. Diamond**[1,2]

[1]*Cognitive Neuroscience Sector, International School for Advanced Studies, 34014 Trieste, Italy, and* [2]*Department of Biomedical Sciences and Technologies, University of Udine, 33100 Udine, Italy*

Rats use their facial vibrissae ("whiskers") to locate and identify objects. To learn about the neural coding of contact between whiskers and objects, we investigated the representation of single-vibrissa deflection by populations of cortical neurons. Microelectrode arrays, arranged in a geometric 10×10 grid, were inserted into the thalamo-recipient layers of "barrel cortex" (the vibrissal region of somatosensory cortex) in urethane-anesthetized rats, and neuronal activity across large sets of barrel-columns was measured. Typically, 5 msec after deflection of a whisker a 0.2 mm^2 focus of activity emerged. It rapidly expanded, doubling in size by 7 msec, before retracting and disappearing 28–59 msec after stimulus onset. The total territory engaged by the stimulus ranged from 0.5 to 2.9 mm^2 (2–11 barrels). Stimulus site dictated the domain of activity. To quantify the coding of whisker location, we applied the population *d′* measure of discriminability. Activity patterns elicited by two whiskers were highly discriminable at the initial cortical response; peak discriminability typically occurred within 16 msec of stimulus onset. To determine how widely information about stimulus location was distributed, we measured population *d′* while excluding response data from the on-center electrodes of the two tested whiskers. Response patterns remained discriminable, indicating that information about stimulus location was distributed across barrel cortex. Taken together, these results show that single-whisker deflections are represented in a multicolumn region constrained by barrel cortex map topography. The nature of this coding allows information about stimulus location to be coded extremely rapidly and unambiguously by one to two spikes per neuron.

Key words: cerebral cortex; electrophysiology; neurons/physiology; vibrissae; discriminability; barrel-column; population coding; multi-electrode

The primary auditory, visual, and tactile cortical regions process sensory inputs in the framework of a large set of columnar, functional modules (Mountcastle, 1997). Although decades of work have provided insights into how individual columns process and redistribute their afferent inputs (Fitzpatrick, 1996), it remains unclear how multiple columns might operate, in parallel, on even the simplest afferent signal. For example, to what extent does the elaboration of information about one stimulus event across multiple columns increase the reliability of the overall cortical representation of the event? A good experimental model for this question is the vibrissal region of rat somatosensory cortex (SI). Layer IV of vibrissal SI is organized as a map of "barrels"(Woolsey and Van der Loos, 1970; Jensen and Killackey, 1987); neurons in a given barrel and its associated column ("barrel-column") yield the strongest response to one single whisker and a weaker response to several surrounding whiskers (Simons, 1978; Armstrong-James and Fox, 1987; Diamond et al., 1993).

The implication from these studies, then, is that the population of neurons participating in the representation of one whisker is distributed spatially across multiple barrel-columns. Although there have been attempts to "reconstruct" population responses on the basis of the synthesis of data from sequentially studied single neurons (Armstrong-James et al., 1992), there are several shortcomings in this approach. The role of trial-to-trial response covariance across the neuronal population cannot be assessed. To sample a large number of single units, many experimental subjects must be used. Differences in anesthetic depth within and between subjects could result in neurons being sampled under different conditions. Delivering small numbers of stimuli to each whisker speeds data collection but can lead to sampling error in some calculations. Moreover, irregular spatial distribution of electrode penetrations makes it difficult to reassemble responses collected at different recording sites. Previous studies that used small arrays of up to 16 electrodes (Ghazanfar and Nicolelis, 1999; Lebedev et al., 2000) failed to sample the full set of responding columns.

Many of these concerns can be addressed because of recent advances in methodology. With the use of the Utah intracortical microelectrode array, neural events are collected simultaneously at 100 microelectrodes laid out in a geometric grid (Harris et al., 1999; Rousche et al., 1999). The distance between adjacent electrode tips is 400 μm, similar to the diameter of a barrel-column in rat cortex. Each cortical column within the territory underlying the array is sampled by at least one microelectrode. This method offers the advantage of conserving the temporal relationships among neuronal spike trains and the spatial relationships among the neurons emitting the spike trains—it is thus well suited to the construction of stimulus-evoked cortical neural activity maps. Here we use the Utah array to reveal the temporal unfolding of barrel cortical neural activity maps in response to single-whisker deflections. We then apply the *d′* measure of signal detection theory to estimate the discriminability—as a function of time—between the activity patterns evoked by whiskers. We interpret the findings in relation to the tactile capacities of the behaving rat.

MATERIALS AND METHODS

Subjects and experimental protocols. One advantage of using the 100-electrode recording array is that the large quantity of data collected in each subject reduces the number of experiments required. In the present study only three subjects were necessary to verify the consistency of all of the main results; see Table 1.

Details on experimental methodology are given in Rousche et al. (1999). All procedures conformed to National Institutes of Health and international standards concerning the use of experimental animals. Adult male Wistar rats weighing 275–400 gm were used. Anesthesia was induced by urethane (1.5 gm/kg of body weight, i.p.). During the recording session body temperature was maintained near 37.5°C, and anesthetic depth was

Table 1. Consistency of principal results across subjects

Experiment	Evoked spikes per stimulus median (IQR)	Number of responding electrodes median (IQR)	Response onset latency median (IQR)	Response offset time mean (SD)	Peak d' mean (SD)
r28	6.0 (4.3–10.3)	14 (8–15)	8 (5–8)	45.8 (19.0)	4.8 (1.0)
r30	4.6 (2.6–5.7)	10 (7–12)	6 (5–17)	44.0 (12.4)	3.4 (0.9)
r32	6.0 (3.3–6.0)	13 (10–13)	9 (7–12)	40.6 (9.3)	3.3 (0.7)
ALL	5.7 (3.3–8.1)	12 (8–15)	8 (6–12)	43.9 (15.1)	4.3 (1.2)

Response latency and response offset time in msec. Standard deviation, SD; interquartile range, IQR.

held at a consistent level by monitoring hindpaw withdrawal, corneal reflex, and respiration rate. Supplemental doses of urethane (0.15 gm/kg) were administered as necessary. With the subject placed in a stereotactic apparatus (Narashige, Tokyo, Japan), the left somatosensory cortex was exposed by a 7-mm-diameter craniotomy centered on a point 2 mm posterior to bregma and 6 mm from the midline. The dura mater was left intact.

The array (Bionic Technologies, Salt Lake City, UT) consisted of a 10×10 grid of 1.0- or 1.5-mm-long electrodes with a 400 μm inter-electrode distance. Electrode array fabrication is described in Jones et al. (1992). The vibrissal region of left somatosensory cortex was identified according to vascular landmarks and stereotactic coordinates (Hall and Lindholm, 1974; Chapin and Lin, 1984), and the array was positioned with the electrode tips, perpendicular to the surface of cortex, pressing very lightly against the dura at the target location. Then it was implanted by using a pneumatic impulse inserter (Bionic Technologies) (Rousche and Normann, 1992) such that the electrodes tips reached those layers receiving afferents from the ventroposterior nucleus of the thalamus, i.e., layer IV and the lower part of layer III (Lu and Lin, 1993). A wire positioned in the cortex served as a reference. From photographs of the inserted arrays, the minimum and maximum depths of electrode penetration were found to be 400 and 900 μm. Figure 1*B* illustrates one case.

Array placement was examined in histological sections. At termination of the recording session the subjects were perfused with saline and 4% paraformaldehyde. After post-fixation in 20% sucrose, the cortex was removed, flattened, and frozen. The block of tissue was cut in 40 μm sections in the tangential plane and stained with cresyl violet.

Electrophysiological data acquisition. Individual whiskers were stimulated 3 mm from their base by a piezoelectric wafer (Morgan Matroc, Bedford, OH) that was controlled by a voltage-pulse generator (A.M.P.I., Jerusalem, Israel). The stimulus, an up–down step function of 80 μm amplitude and 100 msec duration, was delivered at 1 Hz.

Initially, each macrovibrissa (A_{1-4}, B_{1-4}, C_{1-5}, D_{1-5}, E_{1-5}, α, β, γ, and δ) was stimulated 50 times. The subset of whiskers for which the barrel-columns were penetrated by the array received a greater number of stimulus trials (279–500). Whiskers for which the barrel-columns lay at the edge of the array and for which the representations hence would have been sampled incompletely, were excluded from further analysis. The present results are based on the responses to 33 whiskers (rat *r28*: A_{1-2}, B_{1-4}, C_{1-4}, D_{1-3}, and E_{1-3}; rat *r30*: C_{1-3}, D_{1-3}, and E_{1-2}; rat *r32*: C_{1-4}, D_{1-3}, and E_{2-3}).

The data acquisition system (Bionic Technologies) (Guillory and Normann, 1999) consisted of a 100-channel amplifier (gain = 5000, filtered at bandpass 250–7500 Hz), a digital signal processor (DSP), and Pentium PC. Voltage thresholds for each channel were set by using the PC. The DSP detected when the signal on any channel crossed threshold. It then extracted 1.5 msec of analog signal (0.5 msec before the threshold crossing, 1.0 msec after) and digitized it at 30,000 samples/sec per channel. Digitized waveforms were transmitted to the PC for storage. In off-line analysis, spike-sorting programs were used to select the activities of multiple single units on each electrode. Waveforms characteristic of thalamic afferents [initial negative deflection with short duration and high spontaneous activity (Simons and Carvell, 1989)] were recorded rarely and, if encountered, were excluded by spike sorting. To reduce the bias introduced by the selection of single neurons (i.e., to eliminate the decision of which units to "discard" when constructing the whole-array response maps; see below), we summed the neural waveforms of the multiple neurons recorded on each electrode to form a *neural cluster*. That is, the multiunit activity on a given electrode was treated as a single composite unit (for details, see also Rousche et al., 1999).

Analysis of neuronal responses. The first step was to form peristimulus time histograms (PSTHs) by using neural data collected at each electrode across all trials for a given stimulus site. For the purposes of illustration, neural data from all electrodes were used to form whole-array response maps (see Figs. 2*B*, 3, 6). However, for the quantification of cortical response parameters (see Figs. 4, 5, 7), only those electrodes at which the neural cluster gave a statistically significant response were included. *Responding electrodes* were identified by comparing the trial-by-trial post-stimulus (0–100 msec) and prestimulus (−100 to 0 msec) multiunit spike counts, using the Wilcoxon signed ranks test ($p < 0.01$ accepted as a significant response).

On the basis of the observation that the principal whisker of a given barrel-column evokes the greatest response, we estimated the columnar location of each electrode (Ghazanfar and Nicolelis, 1999) (see also Lebedev et al., 2000). An electrode was defined as being in the barrel-column of a given whisker if that whisker elicited a statistically significant response (0–100 msec) that was at least 50% greater than that to all other whiskers. It was also useful to classify the set of electrodes responding to a given whisker as being "on-center" or "off-center." For a specific whisker, an electrode was designated as "on-center" if the response to that whisker was 66% or more of the maximum evoked at that electrode for any whisker. The set of off-center electrodes for a given whisker was simply the set of all responding electrodes that were not on-center.

For all responding electrodes the response onset latency was calculated by using a method similar to that of Maunsell and Gibson (1992). The PSTH was constructed with 1 msec bins from −100 to +100 msec (stimulus onset = 0 msec). Onset latency was defined as the earlier of the first two consecutive poststimulus bins of the PSTH in which the spike count exceeded ($p < 0.01$) the count that would be expected from a Poisson process with mean spike count equal to that of spontaneous firing. Rate of spontaneous firing was determined from the 100 msec interval preceding stimulus onset. Because the rising phase of the PSTH was very sharp (see Fig. 4*A*), latency measurement was relatively insensitive to the critical p value that was chosen. However, response latency is somewhat sensitive to the number of trials, as is the Wilcoxon test of response magnitude. These measurements were always based on 279 stimulus trials (the minimum number used in any experiment) to make them comparable across all whiskers of each rat. The bias attributable to using small numbers of trials was evaluated by repeating the latency analyses on randomly chosen subsets of 50 trials.

To enable comparison with published data, we also estimated modal latencies, using the method of Armstrong-James and Fox (1987). The analysis was restricted to those cases for which the onset latency was well defined. By measuring the time to first spike after stimulus onset on every trial, we constructed a first-spike time histogram with 1 msec bins in the interval 0–100 msec poststimulus. The modal latency was defined as the mode of this histogram.

Discriminability of cortical population response patterns. To determine the discriminability among the neural responses to different whiskers, we adapted the signal detection measure d' (Green and Swets, 1966). d' quantifies how discriminable two events are, based on responses to them. For a single dependent response variable, d' is simply the absolute difference between the mean responses to the two events divided by the average SD. In the present case the events are stimuli presented to two different whiskers, and the dependent response variable is the spike count at an electrode of interest. If the mean values of response for stimuli x and y are m_x and m_y, respectively, and if the SD across both stimuli is σ, then:

$$d' = \frac{|m_x - m_y|}{\sigma}. \tag{1}$$

This measure has been used to study how well single sensory neurons discriminate among relevant stimulus features (Tolhurst et al., 1983; Essick and Whitsel, 1985).

When more than one response variable is available, it is necessary to consider possible covariation among them across trials. If the responses to a given stimulus are statistically independent, then the *population* d' is simply the square root of the sum of the squared individual response d's (Green and Swets, 1966):

$$d' = \sqrt{\sum_i d'^2_i}, \tag{2}$$

where d'_i is the discriminability at the ith response variable (electrode). Equation 2 also has been applied to sequentially recorded neurons, where no information about covariance was available (Zohary, 1992; Geisler and Albrecht, 1997). However, neocortical neurons are not, in general, statistically independent (Gawne and Richmond, 1993; Zohary et al., 1994; Lee et al., 1998). For a given set of stimuli the response covariance can constitute either redundancy or synergy (Snippe, 1996; Oram et al., 1998; Abbott and Dayan, 1999), in which case Equation 2 will overestimate (for redundancy) or underestimate (for synergy) the true discriminability.
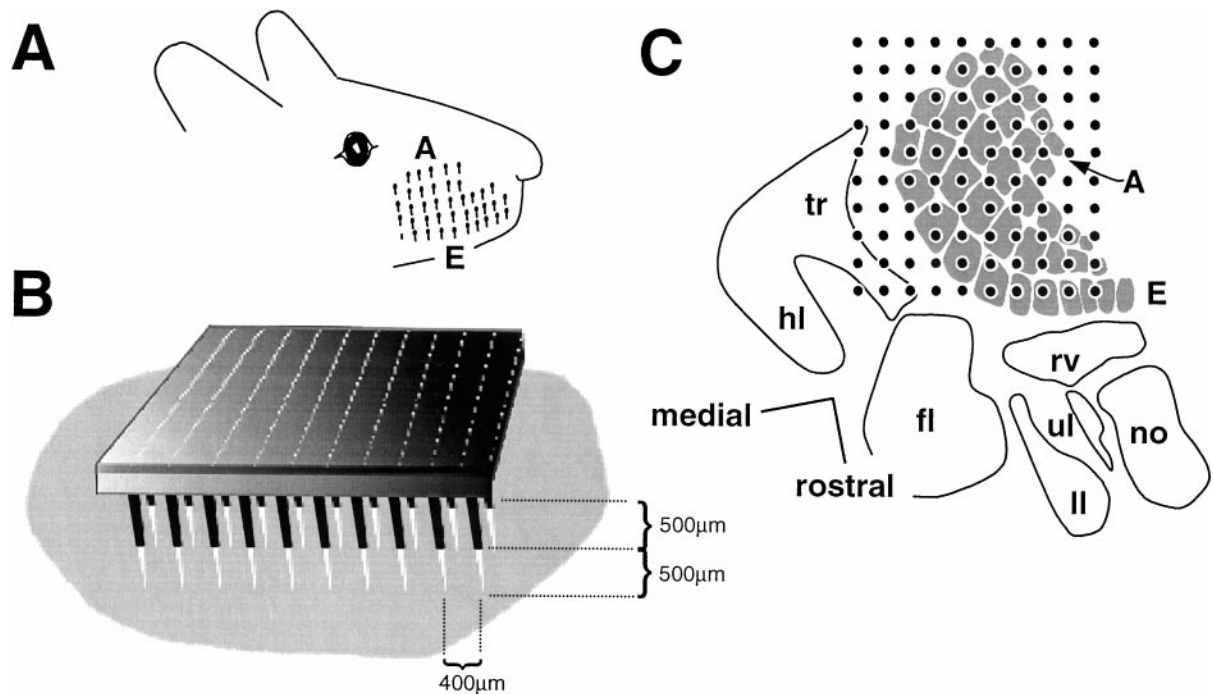
Figure 1. Sampling of the cortical vibrissal representation with a 10 × 10 electrode array. *A*, Disposition of the whiskers (shown as *stubs*) on the snout. *Rows* are labeled with *letters A* (dorsal) to *E* (ventral). *B*, Array position for rat *r30* based on a photomicrograph of the preparation. *Light gray shading* is the dura mater exposed by the craniotomy. A 500 μm length of the electrodes is visible (shown in *black*), and the remaining 500 μm length (shown in *white*) is implanted in the tissue. *C*, Placement of the 10 × 10 microelectrode for rat *r28*. A barrel map was drawn from a nitric oxide synthetase-labeled tangential section (Valtschanoff et al., 1993) and used as a template. Then an electrode grid template was positioned to give the best fit to the physiological data; i.e., each electrode was ascribed the columnar location that matched its principal whisker (see Materials and Methods). *tr*, Trunk; *hl*, hindlimb; *fl*, forelimb; *ul*, upper lip; *ll*, lower lip; *no*, nose; *rv*, rostral vibrissae.

Following the arguments of Green and Swets (1966), the generalization of Equation 2 that takes covariance into account is:

$$d' = \sqrt{(m_x - m_y)^T C^{-1}(m_x - m_y)}, \quad (3)$$

where m_x and m_y are mean response vectors across all electrodes, C is the matrix of covariances between pairs of electrodes, and ^{T} denotes matrix transposition. In the pattern recognition literature this measure of *population d'* is sometimes known as the Mahalanobis distance (see Duda and Hart, 1973).

In practice, means and covariances must be estimated from data. If there are electrodes at which neurons do not respond or respond very weakly, then the inverse covariance matrix can become subject to serious sampling error. In our case this problem was avoided in large part by repeating each stimulus many times (279–500 trials per whisker) and by restricting the analysis to electrodes for which the neurons yielded a significant response. Thus, if there were 10 responding electrodes in the 100-electrode array, then m_x and m_y would be 10-dimensional, and C would be 10 × 10. In the few cases in which the covariance matrix remained singular, we computed discriminability in the subspace in which it was invertible (Metzner et al., 1998), using the singular value decomposition (see Strang, 1988):

$$d' = \sqrt{(m_x - m_y)^T Q \Lambda^{-1} Q^T (m_x - m_y)}. \quad (4)$$

Given that C is a $N \times N$ matrix with rank R, then Q is the $N \times R$ matrix for which the columns are the R eigenvectors of C with non-zero eigenvalue, and Λ is the $R \times R$ diagonal matrix of corresponding eigenvalues.

Bias is another issue that arises when estimating d' from a finite set of data. Suppose that the identical stimulus is delivered across two sets of trials. Ideally, the discriminability between the two sets of responses would be zero. In practice, however, the difference between the two sample mean responses inevitably will be non-zero, resulting in a non-zero value of d'. In this light, it was important to estimate the *chance d'* value obtained by comparing response sets taken from the *same* stimulus. This was accomplished by randomly assigning the responses obtained for a given stimulus to two sets and estimating d' between these two sets. The procedure was repeated 10 times for each stimulus site, yielding estimates for the mean and SD of the chance d'. Thus, for each pair of stimulus sites a true d' estimate and two separate chance d' values were obtained (see Fig. 7A). Finally, the significance of the true d' was evaluated by computing z scores.

RESULTS

Cortical population response to a single whisker

The vibrissae of the snout are arranged in rows A–E, readily identifiable in all subjects (Fig. 1A), and neighborhood relations

among whiskers are conserved in the local topographic relationships among the barrel-columns in contralateral primary somatosensory cortex (Woolsey and Van der Loos, 1970; Welker, 1971). In the present experiments the 400 μm spacing between the electrodes of the array resulted in each column being penetrated by one to three electrodes; a cortical column lying within the array grid was never excluded (Fig. 1C).

In each of the three experiments the neurons residing in ~20–30 cortical columns were recorded. This permitted us to generate maps representing the spatial distribution of the cortical population response as a function of stimulus site. Figure 2, *A* and *B*, illustrates the method by using rat *r28* as an example. Vibrissa C_1 was stimulated 279 times, and a PSTH with 2 msec bins was generated at each electrode for the interval from 40 msec before, until 40 msec after, stimulus onset. All 100 PSTHs are illustrated in Figure 2A. Those electrodes for which neurons gave the largest response are evident by the peak values in the PSTHs. Response magnitude evoked at each electrode was calculated as the average spike count for the 40 msec interval after stimulus onset minus the average spike count in the 40 msec prestimulus interval. In Figure 2B, these values have been plotted at the corresponding electrode positions, on a color scale, to create a "response map." The total number of responding electrodes was 14 (see Materials and Methods for statistical criteria).

To learn about the unfolding of the cortical response over time, Figure 3 (*top*) illustrates neuronal activity in sequential 2 msec segments after upward deflection of whisker C_2 in rat *r32*. In the time window 4–6 msec after stimulus onset, the cortical response emerged as a small central core focused on one electrode. In the time windows 8–10 and 10–12 msec after stimulus onset, the zone of activation expanded laterally to include an area of eight electrodes (1.28 mm²). Thereafter, the cortical activation—both in area and in magnitude—diminished rapidly. The low level of activity evident at 14–16 msec persisted until 36 msec after stimulus onset (data not shown). Release of the whisker from the upward position produced a response to "stimulus offset," illus-
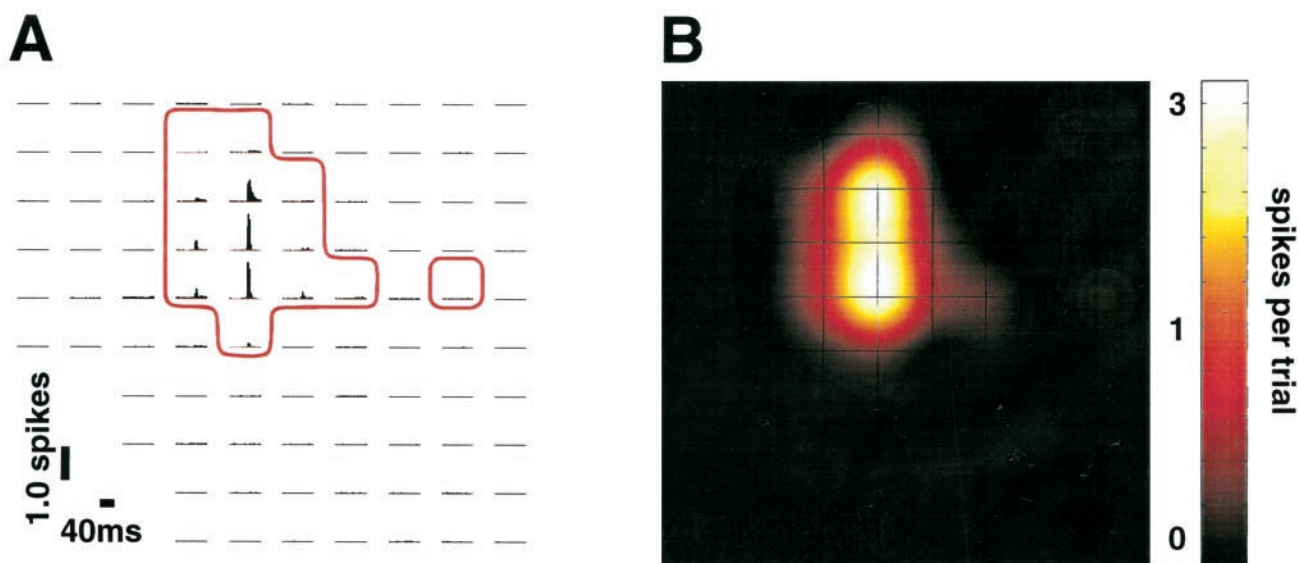
A

B

Figure 2. Cortical response to single whisker deflection. *A*, PSTH map for deflection of whisker C_1 (*r28*); responding electrodes are enclosed by the *red boundary*. Orientation of the electrode sites is the same as in Figure 1*C*. *B*, Cortical response map on the basis of the PSTH data of *A*. For the purpose of illustration, a cubic interpolation was performed between electrodes. Activity is plotted on a logarithmic scale.
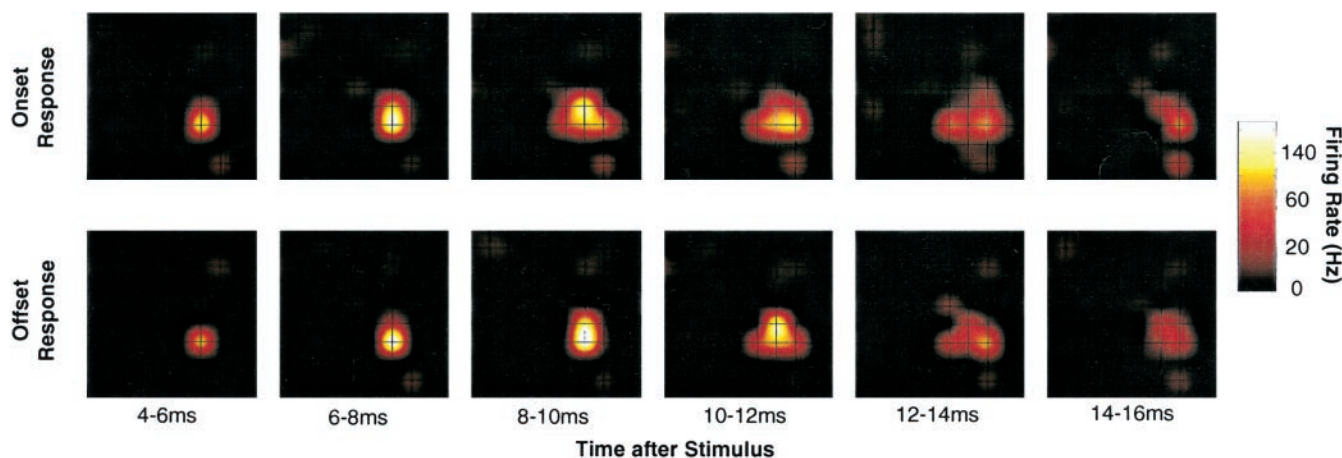

Figure 3. Spatial and temporal features of the cortical response to a single whisker. Data were averaged across 466 stimulus trials delivered to whisker C_2 in rat *r32*. Note the logarithmic scale.

trated in sequential 2 msec segments (Fig. 3, *bottom*). In this example all characteristics (spatial, temporal, and magnitude) of the offset response were similar to those of the onset response. However, stimulus onset was an active deflection of the whisker caused by upward piezoelectric wafer movement, whereas offset was a passive return of the whisker to its resting position. The cortical response to the two kinds of stimulus therefore cannot be compared directly, and the remainder of the paper concerns only the response to stimulus onset.

To provide more detail concerning the spatial and temporal characteristics of the cortical response to stimulus onset, we generated population PSTHs. For each stimulus site the PSTHs at all responding electrodes were summed. The average of these 434 PSTHs from three rats is shown in Figure 4*A*. This composite PSTH reveals an extremely rapid response onset (5 msec) and an early peak in firing rate (8 msec), followed by a gradual dissipation of activity. Barrel cortex firing rate approached the prestimulus level within ~50 msec after stimulus onset. The contributions from on-center and off-center electrodes (see Materials and Methods for definitions) are shown separately in Figure 4*B*. The initial response can be attributed to on-center electrodes. The higher apparent background firing rate for the off-center PSTH is simply attribut-

able to there being more such electrodes than on-center ones for the stimulation of any whisker.

The average number of spikes summated across the neural clusters on all responding electrodes was evaluated for each stimulus site after the count of on-going prestimulus activity was subtracted, and the distribution of whole-array evoked spike counts is given in Figure 4*C*. The interquartile range (IQR) of the distribution is 3.0–8.1 spikes per stimulus trial.

How widely distributed was the response to single-whisker deflection? This was estimated by counting the total number of responding electrodes for each stimulus site. The distribution of electrode counts is given in Figure 4*D*. It is evident that the area activated by individual whiskers was highly variable, ranging from 3 to 18 electrodes. In every experiment the total set of responding electrodes formed a primarily contiguous field that overlaid the barrel field whisker region (see, for example, Fig. 1*C*). Nonresponding electrodes were almost always outside this field in sites lying beyond the whisker representation, e.g., in dysgranular zones (Chapin and Lin, 1990).

From the spatial sampling density of the array we take each electrode to be representative of a 0.16 mm^2 block of barrel cortex. The cortical territory activated by individual whiskers, then, was
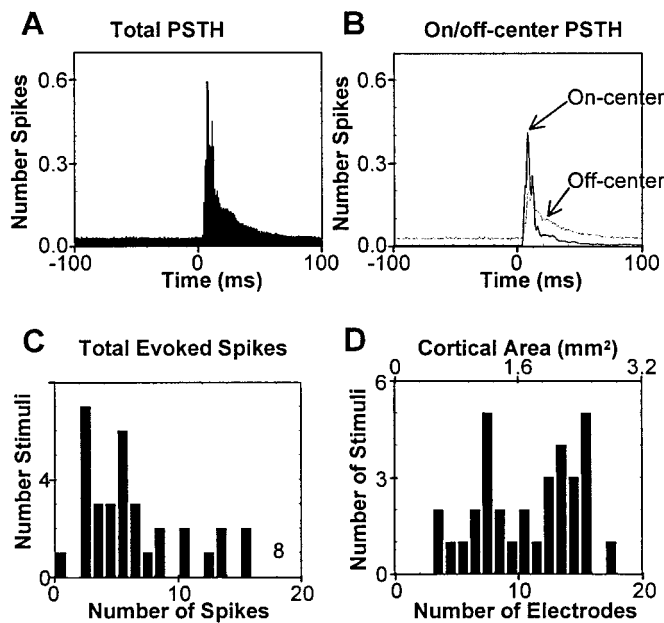
Figure 4. Characteristics of the cortical population response to whisker deflection. *A*, The composite PSTH was formed by summing 434 individual PSTHs across all responding electrodes for all stimuli in all rats. *B*, Composite PSTHs for on-center electrodes (*solid line*) and off-center electrodes (*dotted line*) are shown separately. The sum of these is the total PSTH of *A*. *C*, Histogram of total evoked spikes (across the entire array) per stimulus trial is plotted for the same data considered in *A*. *D*, For each stimulus site the number of responding electrodes was counted; the distribution of electrode counts is shown by using the *bottom scale*. The *top scale* indicates the corresponding cortical area, assuming each electrode to be representative of 0.16 mm^2.

Figure 5. Emergence of the cortical population response. *A*, Onset latencies are mapped onto corresponding electrode positions (rat *r28*, stimulus site B$_1$). Nonresponding electrodes are *black*. The electrode yielding the shortest latency response (6 msec) is indicated by the *bullet*. *B*, Distribution of latencies. The procedure of *A* was repeated for 33 whisker stimuli across three rats; a histogram of all latencies is shown. *C*, The *solid line* shows the expansion of activated cortical territory, averaged over all 33 stimuli. For this analysis an electrode was considered active at all times after its response onset, and cortical territory was derived from the number of electrodes. Error bars denote ±1 SD. The *points* indicate the rate of expansion of the active territory. *D*, The distribution of all response offsets for 33 stimuli.

equivalent to 0.5–2.9 mm^2. The number of distinct barrels activated was 2–11.

Examination of cortical response latency and response duration

The thalamocortical and intracortical pathways through which vibrissal sensory responses are generated has been a subject of debate (Simons and Carvell, 1989; Armstrong-James, 1995; Goldreich et al., 1999). Response timing is one measure used to deduce functional circuitry—for example, the absence of short-latency responses to whiskers other than the "principal" one has been interpreted to mean that barrel neurons do not receive nonprincipal whisker information directly through the thalamic ventral posterior medial (VPM) nucleus (Armstrong-James et al., 1992). By recording signals simultaneously at all electrodes, over a large number of trials, we were able to reexamine this problem with improved reliability. A representative "latency map" (experiment *r28*) is shown in Figure 5*A*. The onset latency to whisker B$_1$ was estimated at each electrode. For any whisker the total set of responding barrel-columns is made up of the topographically matched one and the remainder. With stimulation of whisker B$_1$, neurons at the electrode in the principal barrel-column (marked by the *bullet*) responded at a latency of 6 msec. Neurons at electrodes in several of the immediately adjacent nonprincipal barrel-columns responded at latencies of 7–10 msec, and neurons at electrodes in more distant nonprincipal barrel-columns responded at latencies of 8–16 msec. Clearly, information related to whisker B$_1$ rapidly gained access to a large cortical region. Figure 5*B* illustrates the summary of onset latency data from all responding electrodes for stimulation of all vibrissae in each rat. For a given whisker the neurons at one-half of the responding electrodes became active within 8 msec of stimulus onset (the median value of the distribution). Of course, not all response latencies were short; for 13% of cases the neurons began to respond >20 msec after whisker deflection. For on-center electrodes the median onset latency was 5
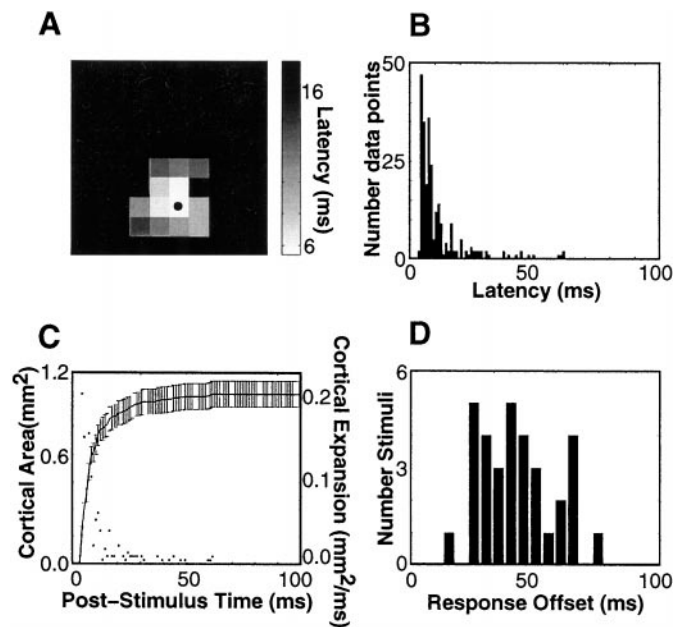
msec, and 97% of observations were <10 msec; for off-center electrodes the corresponding measures were 9 msec and 55%.

For comparison with previously reported data (Armstrong-James and Fox, 1987; Armstrong-James et al., 1992), *modal* latencies were estimated also. In every rat these were significantly longer than the *onset* latencies (Wilcoxon signed ranks; $p < 0.01$). The median value of the total distribution was 12 msec (8 msec for onset latency). For on-center electrodes the median value was 8 msec (IQR, 7–9 msec), and 91% of observations were <10 msec; for off-center electrodes the corresponding values were 13 msec (9–23 msec) and 32%.

The onset latency analysis, coupled with the precise, regular spatial arrangement of the electrodes, allowed us to estimate the total cortical territory activated by a single-whisker stimulus as a function of poststimulus time. Similarly to Figure 4*D*, each electrode was taken to represent 0.16 mm^2 of cortical tissue. Thus, as successive electrodes began to respond after whisker deflection, the active cortical zone grew. This time-dependent engagement of cortical territory is shown by the continuous line in Figure 5*C*, based on the average of all observations. Typically, 5 msec after whisker deflection a territory of 0.2 mm^2 was active, corresponding to the principal barrel-column of the whisker. The activated area expanded very rapidly. By 7 msec, 0.5 mm^2 was active; by 11 msec the active region had grown to 0.9 mm^2. Because the area of a single barrel is ~0.1–0.2 mm^2 (Rice, 1995), this indicates an active domain extending well beyond the principal barrel-column. To check this result, we counted the number of activated electrodes lying in different barrel-columns. By 5 msec the median was one barrel-column (IQR, 1–2), increasing to two (IQR, 1–5) by 7 msec and three (IQR, 1–7) by 11 msec. To facilitate comparison with previous research, we also calculated cortical territories on the basis of modal latencies; the average active territory was 0.1 mm^2 at 5 msec, 0.3 mm^2 at 7 msec, and 0.8 mm^2 at 11 msec.

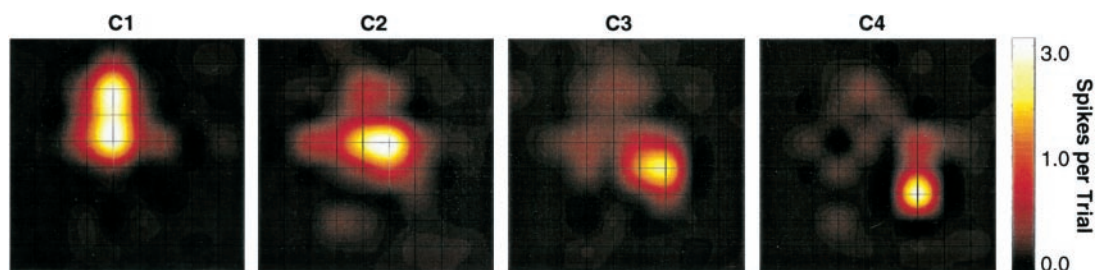To determine the role of the number of trials on latency values,

Figure 6. Projection of whiskers C_1–C_4 onto barrel cortex (rat *r28*). Response maps were generated from the spike count 0–100 msec poststimulus, as in Figure 2*B*.

we repeated the analysis of onset latencies using randomly chosen sets of 50 trials. For each stimulus site we computed the difference in the latency across 279 and across 50 trials. The measured onset latency was slightly longer when only 50 trials were used (median increase, 1 msec; IQR, 0–2 msec). When only on-center electrodes were considered, the median increase was 0 msec (IQR, 0–1 msec). Thus, the small number of trials yields a later response onset at off-center electrodes.

The rapid time course of response onset suggests an anatomically direct thalamocortical route from one whisker to a relatively large area encompassing multiple barrel-columns. However, intracolumnar and intercolumnar circuits undoubtedly contribute to the subsequent processing of sensory information (Armstrong-James et al., 1993). The total duration of the cortical response reflects both "early" thalamocortical and "late" intracortical contributions. To quantify the total response duration, we measured the *response offset* as the time by which 90% of the total number of evoked spikes had occurred. A histogram of response offset for 33 different stimulus sites is shown in Figure 5*D*. The mean offset was 43.4 msec; the SD was 15.1 msec. For 32 of 33 cases the cortical response endured for >20 msec after initial response onset.

Cortical response patterns and discriminability of stimulus site

Once the main features of the cortical response to a single whisker have been characterized, the next step is to determine how these features contribute to the coding of stimulus location. Cortical response patterns evoked by stimulation of whiskers C_1, C_2, C_3, and C_4 (rat *r28*) are shown in Figure 6. One whisker activated a cortical field corresponding to the on-center barrel-column and a set of surrounding barrel-columns. The location of cortical activity was related to stimulus site, as one would predict on the basis of the well known barrel map (Woolsey and Van der Loos, 1970). Still, many neural clusters were in common to the different response patterns, suggesting that a given cortical site participated in the coding of several stimuli. Because it is known that a rat can behave differently depending on which of two neighboring whiskers contacts an object (Harris et al., 1999), it is important to determine how information about stimulus site is encoded. In other words, to what degree do the spatial and temporal parameters of cortical response patterns serve to *separate* the representations of different whiskers? And, how *quickly* does this information become available?

To answer these questions, it was necessary to quantify how reliably two stimuli could be discriminated on the basis of the neural responses. One strategy commonly applied to electrophysiological signals recorded at *single* electrodes is the d' measure of signal detection theory (Tolhurst et al., 1983; Essick and Whitsel, 1985; Parker and Newsome, 1998). To study ensembles of neurons, Zohary (1992) and Geisler and Albrecht (1997) used *population d'*. These papers did not, however, take correlations between simultaneously recorded neurons into account. Here, we use a *population d'* that uses covariance information (see Materials and Methods).

Using the data illustrated in Figure 6, we calculated d' for one pair of whisker-evoked patterns (Fig. 7*A*). Figure 7*A* (*circles, top trace*) shows the time course of discriminability for C_2 versus C_3 in *r28* on the basis of cumulative responses in 4 msec steps: i.e., 0–4,
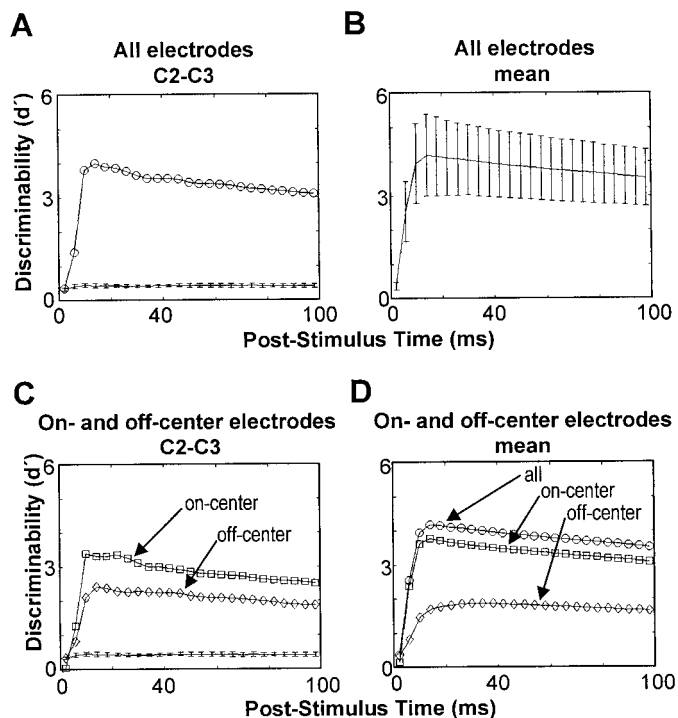

Figure 7. Discriminability between cortical response patterns. *A*, Population d' was estimated for the cortical response to C_2 versus C_3 in rat *r28* in cumulative time bins (*top trace*). The estimated chance d' is shown also (*bottom trace*). The error bars are ±1 SD of the chance d'. *B*, Average population d' across all pairs of stimuli in three rats. The error bars are ±1 SD. *C*, The population d' was estimated for the same stimulus pair shown in *A*, but we used only on-center electrodes (*squares*) or only off-center electrodes (*diamonds*). *D*, Average population d' (*circles*) is compared with the average when only on-center electrodes are used (*squares*) and when only off-center electrodes are used (*diamonds*).

0–8, 0–12 msec, *etc.* The bottom trace is the expected chance d' (error bars denote ±1 SD; see Materials and Methods). At 4 msec poststimulus the discriminability was at chance level; by 8 msec it was above chance. At 16 msec after stimulus onset it had reached its maximum value of 4, after which discriminability declined. Figure 7*B* shows d' averaged over all 184 stimulus pairs, together with the SD. The median time at which d' reached its peak was 16 msec; the IQR was 16–28 msec. It was very common, therefore, for spikes occurring >16 msec after stimulus onset to contribute no information about stimulus location (on average, 32% of evoked spikes occurred later than 16 msec).

If the representation of single whiskers was strictly topographic, d' would depend exclusively on activity in the two barrel-columns topographically matched to the two stimulated whiskers. If, on the other hand, the representation was distributed, there also would be a significant contribution from nonprincipal barrel-columns. To distinguish between these possibilities, we took on-center electrodes to correspond to principal barrel-columns. Then, we com-

pared d' derived from all responding electrodes (Fig. 7*A,B*) with that derived only from off-center electrodes (Fig. 7*C,D*). Figure 7*C* shows the result for the same data used in Figure 7*A*, but with only off-center electrodes (*diamonds*). The peak discriminability decreased from 4.0 to 2.4 but remained well above chance. Indeed, for 183 of 184 stimulus pairs the peak discriminability exceeded the chance level by at least 4 SD even after the removal of on-center electrodes. This means that the activity present at off-center barrel-columns as a group remains capable of supporting the discrimination between this pair of whiskers. On average (Fig. 7*D*), by excluding on-center electrodes, peak discriminability decreased from 4.3 (*circles*) to 1.9 (*diamonds*), and the peak was delayed (30 msec as opposed to 16 msec poststimulus).

Perhaps a more ecologically relevant question is whether activity at off-center electrodes actually improves the reliability of stimulus localization. To find out, we repeated the analysis using only on-center electrodes. On-center electrodes alone supported good discriminability (*squares* in Fig. 7*C,D*), but peak d' was, on average, 10% lower than when off-center channels also were included (compare *circles* with *squares* in Fig. 7*D*). This comparison also indicated that the initial rapid rise in discriminability 0–8 msec after stimulus onset was attributable to on-center electrodes. The spread of single-whisker activity to off-center barrel-columns thus provided a modest increase in reliability of the coding for the stimulus site.

DISCUSSION

Principal findings
By using a large array of 100 closely spaced electrodes covering 13 mm^2, we recorded simultaneously from a large portion of whisker-related SI. Previous investigations concerning the spatial distribution of activity either have attempted to reconstruct the cortical response from sequentially recorded single units (Armstrong-James et al., 1992), or have used small arrays covering 0.6 mm^2 (Ghazanfar and Nicolelis, 1999). Our method enabled us to sample the time course of activity in each of 20–30 contiguous cortical barrel-columns, guaranteeing coverage of the entire region related to a subset of whiskers. The simultaneous recording also permitted us to study population coding without having to assume statistical independence between neurons, as usually is done.

To explore the population coding of stimulus site, we examined whisker discriminability by using the d' measure of signal detection theory. The relevant information begins to be present in somatosensory cortex some 5 msec after deflection of the whisker, allowing an appropriate behavior to be initiated rapidly. Discriminability between pairs of whisker-evoked response patterns was highly robust as early as 8 msec after stimulus onset and was maximal at 16 msec. It is the early cortical response, therefore, that supports discriminability. Off-center barrel-columns do contribute to stimulus discriminability, but much less, and more slowly, than do on-center barrel-columns. Discriminability is accounted for in large part by on-center barrel-columns, but reliability of the discrimination is improved by ~10% as a result of the distribution of activity across multiple barrel-columns.

Cortical response patterns and the underlying circuitry
Single-whisker deflection activated 2–11 barrel-columns lying within a cortical territory of 0.5–2.9 mm^2. The average initial activation encompassed 0.2 mm^2 (one barrel-column) at 5 msec and expanded extremely rapidly. In 50% of cases at least three different barrel-columns were activated within 10 msec of stimulus onset.

Armstrong-James and colleagues (Armstrong-James and Fox, 1987; Armstrong-James et al., 1992, 1993) found modal latencies to principal whisker stimulation in the IQR of 7–11 msec [Armstrong-James et al. (1992), their Fig. 7]. Consistent with this, we found on-center latencies in the range of 7–9 msec. This confirmation is expected, given that our experimental conditions were similar.

However, there is a key difference regarding results for nonprincipal whisker stimulation. Armstrong-James and Fox (1987) reported that 40% of layer IV neurons had a modal response latency

$<$10 msec for principal whisker stimulation, whereas $<$2% had a modal response latency $<$10 msec for nonprincipal whisker stimulation. These data were interpreted to mean that responses to nonprincipal whiskers originate in corticocortical rather than thalamocortical connections. In contrast, our results support the idea that responses to nonprincipal whiskers can be driven by direct VPM inputs; within 10 msec of stimulus onset a cortical territory of some 0.9 mm^2 (1–7 barrel-columns) was activated. We attribute the discrepancy to a combination of factors. First, to detect the fastest existing pathway to cortex, we measured onset latency. Modal latency values for the same data are slightly longer. Second, any latency measurement is sensitive to the number of trials used to estimate it (Maunsell et al., 1999). If insufficient trials are used, the latency will be biased upward; we found that the 50 trials commonly used in previous work could account for an upward bias of ~1 msec for nonprincipal whiskers. Third, our measurements were based on cluster recordings of one to five units (Rousche et al., 1999); this means that each electrode was more likely to have sampled a short-latency neuron than would be the case with single-unit recording. We believe that these three factors can account for the discrepancy with previous data.

In contrast to some earlier claims, therefore, it seems that there is a direct, thalamic route by which surround-receptive fields are generated in the middle cortical layers—as originally suggested by Simons and Carvell (1989). Because essentially all VPM fibers terminate in the topologically corresponding barrel (Jensen and Killackey, 1987; Lu and Lin, 1993), the fast cortical response almost certainly does not result from the divergence of VPM axons. A more likely explanation lies in the fact that individual VPM neurons respond to multiple whisker inputs at short latency (Armstrong-James and Callahan, 1991; Diamond et al., 1992); in other words, VPM surround-receptive fields are transmitted to cortex. This conclusion is consistent with the recent observation that surround-receptive fields persist after barrel lesions; e.g., barrel E_2 neurons continue to respond to deflection of whisker E_1 despite the destruction of barrel E_1 (Goldreich et al., 1999).

Intercolumnar cortical pathways—if not the unique circuitry for the generation of activity in off-center columns—undoubtedly summate with fast thalamocortical pathways to govern the overall distribution of activity. Subsequent to response onset, the responding cortical field widens, typically for an additional 10–30 msec, before gradually diminishing in both size and intensity. When the entire response period is considered, individual whiskers typically are found to engage a field of 3–18 electrodes, corresponding to 0.5–2.9 mm^2 or ~2–11 barrel-columns. A previous attempt to estimate this by using single electrodes yielded six to eight barrels (Armstrong-James et al., 1992). The present experiments do not speak to the question of the spatial and temporal distribution of activity above and below the thalamo-recipient layers but serve as a step in understanding the constraints on cortical sensory processing introduced at the main afferent input stage.

The cortical representation of single whiskers
The activity patterns described in this paper probably do not constitute the *unique* manner in which single-whisker information is represented across barrel cortex. Several factors influence the cortical response to whisker deflection. The type and dosage of anesthetic have a complex relationship with the size of cortical response patterns (Chapin and Lin, 1984; Armstrong-James and George, 1988; Simons et al., 1992; I. Erchova, personal communication). At a given anesthetic level the territory activated by whisker deflection decreases with increasing whisker deflection frequency (Sheth et al., 1998). In awake rats, behavioral conditions play a role (Fanselow and Nicolelis, 1999). Also, rats tend to use their whiskers in concert; in awake rats the response to deflection of any given whisker is influenced by deflections of other whiskers (Brumberg et al., 1996).

Even if our data reflect only one of many possible operating modes of the available sensory system circuitry, the nature of the whisker representation uncovered here seems to agree with evi-

dence from naturally behaving rats. The same fundamental whisker-to-cortex projection we have shown—strong activation of the principal barrel-column and weak activation of surrounding barrel-columns—has been observed with both 2-deoxyglucose metabolism (Chmielowska et al., 1986; Kossut et al., 1988) and *c-fos*/*zif268* expression (Melzer and Steiner, 1997) in freely exploring rats with one whisker intact. Evidence from the "gap-crossing task," a behavior known to depend on the contribution of the barrel cortex (Hutson and Masterton, 1986), also indicates that the processing of information from one whisker is limited to a small territory. We trained rats to perform the task (Harris et al., 1999) with one whisker intact. When subsequently they were tested on the same task with the "trained" whisker clipped and a "prosthetic" whisker attached, there was significant transfer of learning *only* if the prosthetic whisker was attached to the same stub as the trained whisker or to an immediate neighbor. Thus, consistent with the present physiological analysis, the behavioral experiment suggests that the locus of information processing (and learning-induced neural modification) associated with a single whisker is a cortical domain consisting of the topographically matched and the surrounding barrel-columns.

Speed of whisker processing

We found that the peak discriminability between whisker response patterns occurred 16 msec after deflection, on average. Because only a few neurons per barrel-column were sampled and because only information in the time-varying firing rate was considered, this should be considered a conservative estimate. It is likely therefore that, in layers III–IV, information about stimulation site is carried by the spatially focused early cortical response rather than the more diffuse late response. For the d' measure, those spikes occurring later than the time of peak d' can be regarded as contributing only "noise" to the discrimination of stimulus location. In our data set, therefore, activity recorded later than 16 msec poststimulus (32% of all spikes) was noise. During a behavioral task such as gap crossing, where differences in the sensory signal evoked by different whiskers have real behavioral significance (Harris et al., 1999), we suggest that the relevant information in barrel cortex is maximized within 16 msec of whisker contact.

Within such a short time interval any given cortical neuron will have fired at most one to two spikes. The same conclusion—that very few spikes per neuron convey large amounts of information and support sophisticated computation—has been argued to be widely applicable across species and sensory modalities (Rieke et al., 1997). Two examples are face recognition in primates (Thorpe et al., 1996) and motion detection in insects (Bialek et al., 1991). Our data concern the question of stimulus location and should not be taken to imply that *all* peripheral events can be coded at the cortical level by individual spikes in a restricted locus. Temporal patterns of spikes might be crucial for the discrimination of surface texture, for example. The coding of more complicated stimuli is a topic of current research.

REFERENCES

Abbott LF, Dayan P (1999) The effect of correlated variability on the accuracy of a population code. Neural Comput 11:91–101.

Armstrong-James M (1995) The nature and plasticity of sensory processing within adult rat barrel cortex. In: The barrel cortex of rodents (Jones EG, Diamond IT, eds). New York: Plenum.

Armstrong-James M, Callahan CA (1991) Thalamo-cortical processing of vibrissal information in the rat. II. Spatiotemporal convergence in the thalamic ventroposterior medial nucleus (VPm) and its relevance to generation of receptive fields of S1 cortical "barrel" neurones. J Comp Neurol 303:211–224.

Armstrong-James M, Fox K (1987) Spatiotemporal convergence and divergence in the rat S1 "barrel" cortex. J Comp Neurol 263:265–281.

Armstrong-James M, George MJ (1988) Influence of anesthesia on spontaneous activity and receptive field size of single units in rat Sm1 neocortex. Exp Neurol 99:369–387.

Armstrong-James M, Fox K, Das-Gupta A (1992) Flow of excitation within rat barrel cortex on striking a single vibrissa. J Neurophysiol 68:1345–1358.

Armstrong-James M, Welker E, Callahan CA (1993) The contribution of NMDA and non-NMDA receptors to fast and slow transmission of sensory information in the rat SI barrel cortex. J Neurosci 13:2149–2160.

Bialek W, Rieke F, Ruyter van Steveninck RR, Warland D (1991) Reading a neural code. Science 252:1854–1857.

Brumberg JC, Pinto DJ, Simons DJ (1996) Spatial gradients and inhibitory summation in the rat whisker barrel system. J Neurophysiol 76:130–140.

Chapin JK, Lin CS (1984) Mapping the body representation in the SI cortex of anesthetized and awake rats. J Comp Neurol 229:199–213.

Chapin JK, Lin CS (1990) The somatic sensory cortex of the rat. In: The cerebral cortex of the rat (Kolb B, Tees RC, eds), pp 341–380. Cambridge, MA: MIT.

Chmielowska J, Kossut M, Chmielowski M (1986) Single vibrissal cortical column in the mouse labeled with 2-deoxyglucose. Exp Brain Res 63:607–619.

Diamond ME, Armstrong-James M, Ebner FF (1992) Somatic sensory responses in the rostral sector of the posterior group (POm) and in the ventral posterior medial nucleus (VPM) of the rat thalamus. J Comp Neurol 318:462–476.

Diamond ME, Armstrong-James M, Ebner FF (1993) Experience-dependent plasticity in adult rat barrel cortex. Proc Natl Acad Sci USA 90:2082–2086.

Duda RO, Hart PE (1973) Pattern classification and scene analysis. New York: Wiley.

Essick GK, Whitsel BL (1985) Assessment of the capacity of human subjects and S-I neurons to distinguish opposing directions of stimulus motion across the skin. Brain Res 357:187–212.

Fanselow EE, Nicolelis MA (1999) Behavioral modulation of tactile responses in the rat somatosensory system. J Neurosci 19:7603–7616.

Fitzpatrick D (1996) The functional organization of local circuits in visual cortex: insights from the study of tree shrew striate cortex. Cereb Cortex 6:329–341.

Gawne TJ, Richmond BJ (1993) How independent are the messages carried by adjacent inferior temporal cortical neurons? J Neurosci 13:2758–2771.

Geisler WS, Albrecht DG (1997) Visual cortex neurons in monkeys and cats: detection, discrimination, and identification. Vis Neurosci 14:897–919.

Ghazanfar AA, Nicolelis MA (1999) Spatiotemporal properties of layer V neurons of the rat primary somatosensory cortex. Cereb Cortex 9:348–361.

Goldreich D, Kyriazi HT, Simons DJ (1999) Functional independence of layer IV barrels in rodent somatosensory cortex. J Neurophysiol 82:1311–1316.

Green DM, Swets J (1966) Signal detection theory and psychophysics. New York: Wiley.

Guillory KS, Normann RA (1999) A 100-channel system for real time detection and storage of extracellular spike waveforms. J Neurosci Methods 91:21–29.

Hall RD, Lindholm EP (1974) Organization of motor and somatosensory neocortex in the albino rat. Brain Res 66:23–38.

Harris JA, Petersen RS, Diamond ME (1999) Distribution of tactile learning and its neural basis. Proc Natl Acad Sci USA 96:7587–7591.

Hutson KA, Masterton RB (1986) The sensory contribution of a single vibrissa's cortical barrel. J Neurophysiol 56:1196–1223.

Jensen KF, Killackey HP (1987) Terminal arbors of axons projecting to the somatosensory cortex of the adult rat. I. The normal morphology of specific thalamocortical afferents. J Neurosci 7:3529–3543.

Jones KE, Campbell PK, Normann RA (1992) A glass/silicon composite intracortical electrode array. Ann Biomed Eng 20:423–437.

Kossut M, Hand PJ, Greenberg J, Hand CL (1988) Single vibrissal cortical column in SI cortex of rat and its alterations in neonatal and adult vibrissa-deafferented animals: a quantitative 2DG study. J Neurophysiol 60:829–852.

Lebedev MA, Mirabella G, Erchova I, Diamond ME (2000) Experience-dependent plasticity of rat barrel cortex: redistribution of activity across barrel-columns. Cereb Cortex 10:23–31.

Lee D, Port NL, Kruse W, Georgopoulos AP (1998) Variability and correlated noise in the discharge of neurons in motor and parietal areas of the primate cortex. J Neurosci 18:1161–1170.

Lu SM, Lin RC (1993) Thalamic afferents of the rat barrel cortex: a light- and electron-microscopic study using *Phaseolus vulgaris* leucoagglutinin as an anterograde tracer. Somatosens Mot Res 10:1–16.

Maunsell JH, Gibson JR (1992) Visual response latencies in striate cortex of the macaque monkey. J Neurophysiol 68:1332–1344.

Maunsell JH, Ghose GM, Assad JA, McAdams CJ, Boudreau CE, Noerager BD (1999) Visual response latencies of magnocellular and parvocellular LGN neurons in macaque monkeys. Vis Neurosci 16:1–14.

Melzer P, Steiner H (1997) Stimulus-dependent expression of *immediate-early* genes in rat somatosensory cortex. J Comp Neurol 380:145–153.

Metzner W, Koch C, Wessel R, Gabbiani F (1998) Feature extraction by burst-like spike patterns in multiple sensory maps. J Neurosci 18:2283–2300.

Mountcastle VB (1997) The columnar organization of the neocortex. Brain 120:701–722.

Oram MW, Foldiak P, Perrett DI, Sengpiel F (1998) The "ideal homunculus": decoding neural population signals. Trends Neurosci [Erratum (1998) 21:365] 21:259–265.

Parker AJ, Newsome WT (1998) Sense and the single neuron: probing the physiology of perception. Annu Rev Neurosci 21:227–277.

Rice FL (1995) Comparative aspects of barrel structure and development. In: The barrel cortex of rodents (Jones EG, Diamond IT, eds). New York: Plenum.

Rieke F, Warland D, Ruyter van Steveninck RR, Bialek W (1997) Spikes: exploring the neural code. Cambridge, MA: MIT.

Rousche PJ, Normann RA (1992) A method for pneumatically inserting an array of penetrating electrodes into cortical tissue. Ann Biomed Eng 20:413–422.

Rousche PJ, Petersen RS, Battiston S, Giannotta S, Diamond ME (1999) Examination of the spatial and temporal distribution of sensory cortical activity using a 100-electrode array. J Neurosci Methods 90:57–66.

Sheth BR, Moore CI, Sur M (1998) Temporal modulation of spatial borders in rat barrel cortex. J Neurophysiol 79:464–470.

Simons DJ (1978) Response properties of vibrissa units in rat SI somatosensory neocortex. J Neurophysiol 41:798–820.

Simons DJ, Carvell GE (1989) Thalamocortical response transformation in the rat vibrissa/barrel system. J Neurophysiol 61:311–330.

Simons DJ, Carvell GE, Hershey AE, Bryant DP (1992) Responses of barrel cortex neurons in awake rats and effects of urethane anesthesia. Exp Brain Res 91:259–272.

Snippe HP (1996) Parameter extraction from population codes: a critical assessment. Neural Comput 8:511–529.

Strang G (1988) Linear algebra and its applications. San Diego: Harcourt Brace Jovanovich.

Thorpe S, Fize D, Marlot C (1996) Speed of processing in the human visual system. Nature 381:520–522.

Tolhurst DJ, Movshon JA, Dean AF (1983) The statistical reliability of signals in single neurons in cat and monkey visual cortex. Vision Res 23:775–785.

Valtschanoff JG, Weinberg RJ, Kharazia VN, Schmidt HH, Nakane M, Rustioni A (1993) Neurons in rat cerebral cortex that synthesize nitric oxide: NADPH diaphorase histochemistry, NOS immunocytochemistry, and colocalization with GABA. Neurosci Lett 157:157–161.

Welker C (1971) Microelectrode delineation of fine grain somatotopic organization of (Sm1) cerebral neocortex in albino rat. Brain Res 26:259–275.

Woolsey TA, Van der Loos H (1970) The structural organization of layer IV in the somatosensory region (SI) of mouse cerebral cortex. The description of a cortical field composed of discrete cytoarchitectonic units. Brain Res 17:205–242.

Zohary E (1992) Population coding of visual stimuli by cortical neurons tuned to more than one dimension. Biol Cybern 66:265–272.

Zohary E, Shadlen MN, Newsome WT (1994) Correlated neuronal discharge rate and its implications for psychophysical performance. Nature [Erratum (1994) 371:358] 370:140–143.